

Intelligent MPPT control for SEPIC-Luo converter in grid tied photovoltaic system

D. Thivya Prasad¹, R. Anandhakumar¹, P. Balamurugan²

¹Department of Electrical and Electronics Engineering, Faculty of Engineering and Technology, Annamalai University, Chidambaram, India

²Department of Electrical and Electronics Engineering, Mount Zion College of Engineering and Technology, Chidambaram, India

Article Info

Article history:

Received Feb 2, 2023

Revised Jul 3, 2023

Accepted Jul 25, 2023

Keywords:

1 Φ VSI

Cascaded fuzzy MPPT

Grid

Integrated SEPIC-LUO

PI controller

PV system

ABSTRACT

Grid connected solar photovoltaic (SPV) systems are becoming more and more common due to steadily rising energy demand. The advantages of photovoltaic power generation, such as its eco-friendliness, low maintenance requirements, and lack of noise, are making it as a significant renewable energy source (RES). This framework presents the modeling and control design of PV grid tied system implemented with integrated single ended primary inductance (SEPIC) Luo converter. The main goal of this work includes investigating solar PV system behaviour and creating an effective grid connected solar power. Solar PV module tracks maximum power, with an aid of chaotic cascaded fuzzy a maximum power point tracking (MPPT) has developed. The DC voltage obtained is fed to 1 Φ voltage source inverter (VSI) for conversion of AC voltage. In comparison to typical PWM control, the spectrum performance of the examined voltages is improved by adjusting the nominal duty cycle of main switch of SEPIC-Luo converter. So that PV output impedance is equivalent to DC-DC converter's input resistance. Finally, the obtained AC voltage is supplied to 1 Φ grid for further applications. With less THD, an efficiency of 96% is achieved when the implementation of the suggested system is carried out using MATLAB/Simulink.

This is an open access article under the [CC BY-SA](https://creativecommons.org/licenses/by-sa/4.0/) license.



Corresponding Author:

D. Thivya Prasad

Department of Electrical and Electronics Engineering, Faculty of Engineering and Technology,

Annamalai University

Annamalai Nagar, Chidambaram, Tamil Nadu 608002, India

Email: dthivyaaprasad45@gmail.com

1. INTRODUCTION

Due to the importance of non-energy functions of fossil fuel products in industry, high crude oil prices and global environmental challenges, new energy sources have been quickly growing all over world in recent years. The availability of fossil fuels is finite, and their prices are determined by a variety of political and economic factors [1]–[3]. After the oil crisis of late 1970s, the usage of renewable energy in general and solar energy in particular has gradually expanded. This has prompted scientists and decision makers from all over the world to highlight various strategies for more successfully and efficiently harnessing solar energy, particularly in the field of thrust [4]. Solar energy can be used in terrestrial areas in two different ways: one is through the sun thermal route, which uses solar collectors, and dryers by solar photovoltaic (SPV) method [5]. The PV systems require no intermediate sources for its conversion process and are low maintainable, modular, and robust in nature. They possess the self-ability of generating power of higher

ranges. The electrification of rural areas, particularly in developing countries, has been greatly aided by stand-alone photovoltaic system [6]–[8].

Power electronic converters are crucial in an area of renewable energy as they act as a bridge between those sources and electrical grid. When used to their full potential, they increase the power exchange from RES so that necessary output is produced with more efficiency and at a lower cost [9], [10]. A solar PV array's voltage output is often quite modest and is influenced by the temperature and humidity. PV systems are configured in series and parallel utilizing boost converters to attain high output voltage levels, but this causes a loss of effectiveness and a rise in system size. In these voltage boosting situations, a high voltage gain converter is implemented. By altering a duty cycle, the converter rises the voltage at output to significantly higher levels relative to its input [11]–[13]. Buck-boost and Cuk [14] converters offer an option to have output voltage greater or lower than the input among topologies that are accessible. Even though buck-boost architecture is less expensive than Cuk [15], it is less effective due to various drawbacks such discontinuous input current, excessive peak current, and poor transient responsiveness. Cuk and SEPIC [16] converters' massive input current waves continue to have an effect on maximum power point tracking (MPPT) efficiency. This is because PV systems vary substantially in terms of their maximum power point [17]. Luo converter [18], which has features like simple design, producing nearly zero output voltage and ripple current has high boosting efficiency, but possess longer computational time. To overcome the shortcomings of aforementioned DC converter this research proposes, SEPIC-Luo converter, which generate high output voltage for efficient system operation.

Some strategies are put out to remedy the ineffectiveness of PV systems, one of which is a novel idea known as MPPT. The goal of all MPPT techniques is to increase the output power by tracking the maximum power during every operational scenario. There are many algorithms available that track MPPs. Most of them are simpler, such those that rely on current feedback and voltage while others, like an incremental conductance (IncCond) or perturbation and observation (P&O) method [19]–[21] are more challenging. They also differ in terms of their uses, popularity, and operational range, speed of convergence, cost, and capacity to identify numerous local maxima. Moreover, as power change is only believed to be a consequence of perturbation of voltage, P&O approach is unable to correlate this voltage with MPP voltage. In contrast, some MPPTs need specialized design and understanding with particular topics, like fuzzy logic or neural network approaches [22], and are therefore more impressive since they are faster and more accurate. MPPT fuzzy logic controller (FLC) performs well in a variety of atmospheric situations and outperforms P&O control mechanism; nevertheless, the main controversy is that it heavily depends on technical expertise of engineer to calculate error and create rule-based table.

The DC link voltage for converter is applied to 1 Φ voltage source inverter (VSI) [23], for AC voltage conversion. On grid side, voltage is controlled with an assistance of PI [24] controller, which results in generating stabilized voltage for grid applications. In this research, a single-phase inverter topology with high performance for grid connected PV system is proposed. In addition to increasing low photovoltaic array voltage the proposed arrangement tracks maximum power from PV and convert solar DC electricity into high grade AC power for feeding into grid.

2. PROPOSED SYSTEM

The emphasis today is shifting towards incorporation of small and medium sized power plants generated by renewable energies into electrical grid. SPV is the renewable energy source that is rising faster, and PV facilities are connected to distribution system using a 1 Φ VSI. The Schematic configuration of proposed work in depicted in Figure 1. Stringent control requirements apply to the grid integrated inverter. To reduce the harmonics in current injected to grid and to manage power distribution between plant and grid, a control technique is used.

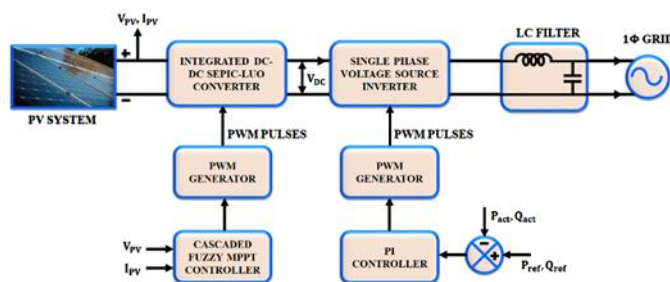


Figure 1. Block diagram of proposed system

An innovative single-stage architecture proposed in this research is appropriate for stand-alone or grid connected PV applications. For a PV system that uses grid, the framework proposes an effective integrated SEPIC-Luo converter with an MPPT approach. The maximum power from PV is tracked utilizing cascaded fuzzy controller approach providing continuous maximum output power obtained from solar irradiance based on temperature. The obtained power is supplied to DC link for feeding a grid. PV voltage is converted into AC with a support of 1 Φ VSI for providing grid supply. It is necessary to use a closed loop PI controller to analyze an error signal and maintain steady state error. Therefore, this system produces less distortion as well as reliable power and grid synchronization.

2.1. Modelling of solar PV system

An architectural foundation for photovoltaic systems has been a silicon p-n junction, which transfers solar energy directly into electrical energy. Electrons are released across the closed electrical circuits once it is exposed to light. Figure 2 illustrates conceptual structure of a photovoltaic system. Higher energy levels are obtained by cells as a result of photon electron collisions as well as for generating current, electrons have the capacity to freely cross the junction. Hence, the level of solar illumination influences a photocurrent I_{pv} generated from photovoltaic cell.

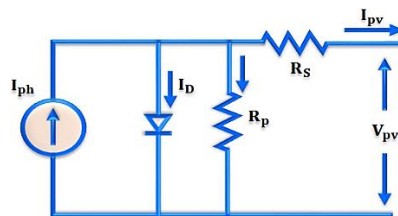


Figure 2. PV system configuration

The PV cell output current (I_{pv}) is represented as the following utilizing Kirchoff's current law as (1).

$$I_{pv} = I_{ph} - I_D - I_{sh} \quad (1)$$

Solar irradiation is inversely correlated with the generated current through photon (I_{ph}). Shunt resistor current is denoted by the symbol I_{sh} and I_D represents diode current. The characteristic equation for PV modules is better expressed as (2) and (3),

$$I_{pv} = C_s I_{ph} - I_D - I_{sh} \quad (2)$$

$$C_p I_{ph} - C_p I_o \left[\exp \left(\frac{q(V_{pv} + R_s I_{pv})}{C_s ZKT} \right) - 1 \right] - \frac{V_{pv} + R_s I_{pv}}{R_{sh}} \quad (3)$$

where I_o specifies saturation current, R_s and R_{sh} as series resistance and shunt resistance, C_s and C_p as no. of cells in series and parallel, output of PV module as V_{pv} , charge of electron as q , identity factor of diode as Z , K as Boltzmann constant, and T as cell temperature. In (4) and (5), I_{ph} and I_o are expressed as (4) and (5).

$$I_{ph} = I_{sc} + K_i (T - T_r) \frac{G}{G_r} \quad (4)$$

$$I_o = I_{sc} \left(\frac{T}{T_r} \right)^3 \exp \left(\frac{q E_{go}}{C_s A Z T} \left(\frac{1}{T_r} - \frac{1}{T} \right) \right) \quad (5)$$

Here, I_{sc} specifies standard test for a photovoltaic module's short circuit current with 1000 W/m² at conduction temperature 25 °C, reference temperature is T_r in Kelvin, K_i indicates the temperature of short circuit current coefficient, G symbolises solar irradiation, I_{sc} denotes 25 °C current saturation, G_r indicates reference solar irradiation and E_{go} represents the band gap.

2.2. Operation of integrated SEPIC-Luo converter

The configuration of the proposed SEPIC-Luo for the purpose of boosting voltage is illustrated in Figure 3(a). The SEPIC-Luo converter can operate efficiently over a wide range of input voltages, including

both step-up and step-down conversion. This makes it suitable for various applications where the input voltage can vary significantly. The converter has two operating modes as presented in Figures 3(b) and 3(c):

- Mode 1: when charging, the anti-parallel diode " D_1 " and switch " S_2 " turned ON. During the charging situation, the circuit arrangement serves as a zeta converter. The typical DC bus voltage, which is higher than the circuit voltage, serves as input voltage during charging, operating similarly to a buck converter. In order to maintain desired voltage at terminal and deliver proper charging current, the duty cycle (D_c) of PWM signal for switch " S_2 " is adjusted. The Luo converter's I-O voltage relationship is stated as,

$$V_{in} = \frac{D_c}{1-D_c} V_{os} \quad (6)$$

- Mode 2: during discharging, the switch S_1 and the anti-parallel diode D_2 are turned ON. Thus, the circuit configuration exhibits SEPIC converter behaviour. Here, the converter serves as boost converter since it raises the voltage to regulated output voltage while feeding the discharged current to DC bus through SEPIC arrangement. The duty ratio (D_d) of PWM signal from switch " S_1 " is used to adjust converter's output voltage (V_{os}), which in turn regulates the discharged current. The input-output relation of SEPIC converter is described as follows while operating at discharging mode:

$$V_{os} = \frac{D_d}{1-D_d} V_{in} \quad (7)$$

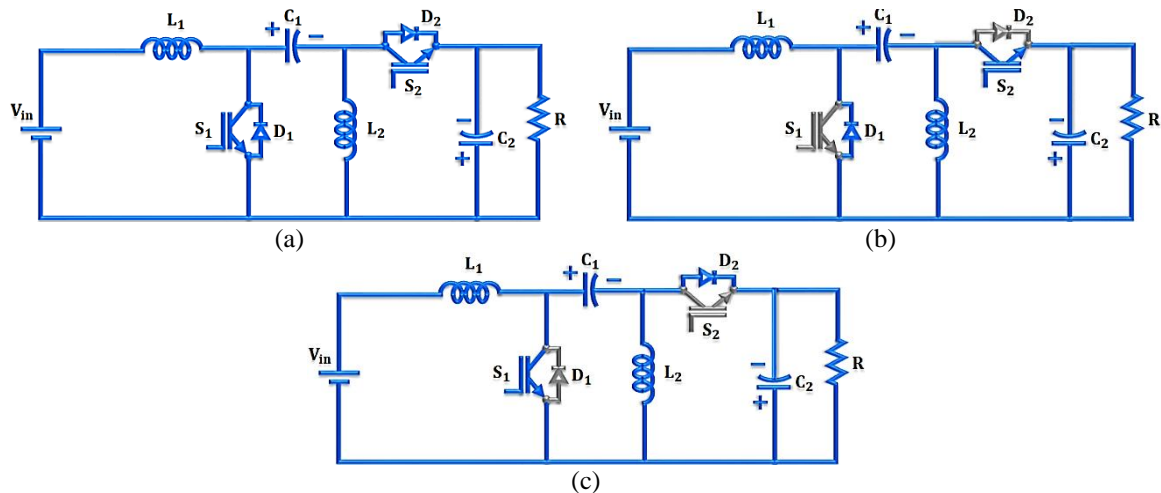


Figure 3. Proposed SEPIC-Luo converter (a) equivalent circuit, (b) mode-1 operation, and (c) mode 2 operation

2.3. Cascaded fuzzy based MPPT algorithm

Contrastingly, with classical controller, it is essential to identify an appropriate mathematical representation of plants, to adjust controller variables and to implement the developed controller into practice. Conventional controllers are not beneficial in nonlinear control applications since majority of actual system function nonlinearly and modelling them is challenging. Alternative control systems including intelligent control, adaptive control or fuzzy logic control have raised significant challenges in an attempt to solve various types of issues as well as possess an efficient tuned controller for entire range of working areas.

Among the finest implementations of fuzzy sets is fuzzy logic controllers. Instead of using numerical variables, they typically employ linguistic parameters as similar to the action of humans. They are beneficial because they can deal with nonlinearities, manage inconsistent inputs, and doesn't require a precise mathematical description of system. Using imprecise or poorly described ideas are permitted under the fuzzy control theory. FLC functions efficiently even when its parameters change and there are outside disruptions due to its nonlinear and adaptable nature. Hence, even under constantly shifting atmospheric circumstances, it provides enhanced MPPT performance. Therefore, for improving an accuracy performance of tracking maximum power a unique approach termed cascaded fuzzy control method.

A cascade fuzzy control technique has been developed which combines an outer as well as inner controller into two cascaded fuzzy controllers. A formal technique is established by fuzzy control to describe,

manipulate and execute domain control knowledge in order to regulate the system. Fuzzy controllers are an innovative and effective alternative to standard control methods due to its intrinsic nonlinearity and capacity for formalize control information as illustrated in Figure 4.

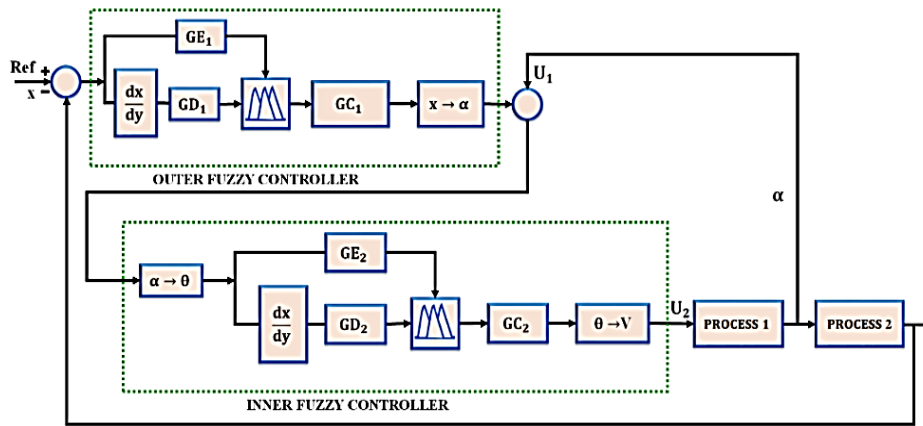


Figure 4. Cascaded fuzzy controller architecture

A combination of following principles results in a fuzzy controller at an outer loop as (8).

$$R^k: E_i \text{ is } A_1^k \text{ and } \Delta E_i \text{ is } A_2^k \text{ then } U_i = B_k \tag{8}$$

Where R^k -kth rule ($k=1, 2, y, m$), E_i denote error, ΔE_i represent change of error, A_1^k and A_2^k are fuzzy set of linguistic values described over related change of error and discourse of error, U_i specifies output and B_k indicates numeric control value.

For both the inner and outer loop, a level of each control rule's activation is calculated using a conventional method.

$$\text{innerloop: } w_{1k} = \min\{\mu_{A_{1k}}(E), \mu_{A_{2k}}(\Delta E)\} \tag{9}$$

$$\text{outerloop: } w_{2k} = \min\{\mu_{A_{1k}}(E), \mu_{A_{2k}}(\Delta E)\} \tag{10}$$

The following is a determination of an inferred values of control in these loops.

$$-U_1^* = \frac{\sum_{k=1}^m w_{1k} B^k}{\sum_{k=1}^m w_{1k}} \tag{11}$$

$$U_2^* = \frac{\sum_{k=1}^m w_{2k} B^k}{\sum_{k=1}^m w_{2k}} \tag{12}$$

Additionally, various scaling factors are applied to the outputs for increasing fuzzy controller's optimization's flexibility.

$$\text{Output of outerloop: } U_1(t) = U_1^*(t)GC_1 \tag{13}$$

$$\text{Output of innerloop: } U_2(t) = U_2^*(t)GC_2 \tag{14}$$

An input variables E and DE have following membership functions which are: NS represents negative small, NM signifies negative medium, NB denotes negative big, PS symbolizes positive small, ZO indicates zero, positive medium is specifies as PM and positive big is illustrated by PB.

The following membership functions comprise the controller's output variable, which represents changes in control including NB (m_3), PS (m_1), NM (m_2), NS (m_1), ZO (0), PM (m_2), and PB (m_3). The membership functions' initial variables are equivalent to m_1 , m_2 and m_3 . Table 1 presents a collection of rules

for a fuzzy controller. A usage of triangular membership functions for fuzzy sets created in an input space is shown in Figures 5(a) and 5(b). PSO has been employed for optimizing membership functions for output parameter. Finally, optimal state of fuzzy cascade controller has been achieved by their changes.

Table 1. Rule base for fuzzy controller [25]

$\Delta E/E$	NB	NM	NS	ZO	PS	PM	PB
NB	$-m_3$	$-m_3$	$-m_3$	$-m_3$	$-m_2$	$-m_1$	0
NM	$-m_3$	$-m_3$	$-m_3$	$-m_3$	$-m_1$	0	m_1
NS	$-m_3$	$-m_3$	$-m_3$	$-m_1$	0	m_1	m_2
ZO	$-m_3$	$-m_3$	$-m_1$	0	m_1	m_2	m_3
PS	$-m_2$	$-m_1$	0	m_1	m_2	m_3	m_3
PM	$-m_1$	0	m_1	m_2	m_3	m_3	m_3
PB	0	m_1	m_2	m_3	m_3	m_3	m_3

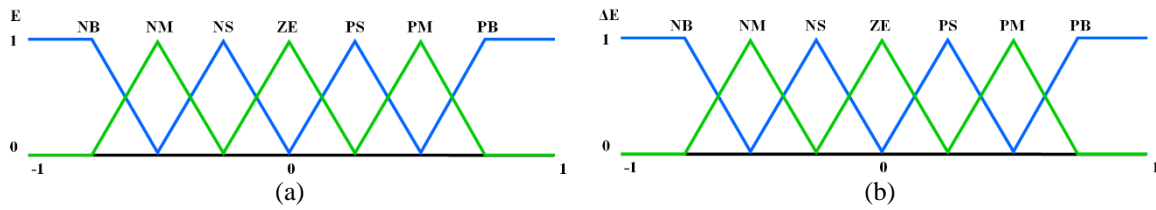


Figure 5. Membership functions for premises parameters (a) membership functions for input E and (b) membership functions for input ΔE

A fuzzy controller in inner loop uses an output of fuzzy system in an outer loop as a reference value. An inner loop's fuzzy controller regulates the system's motor utilising received output from the outer loop. Fuzzy controller modifies an angle of lever arm to the appropriate location by adjusting the motor's position. Hence, by altering the beam's angle, the ball is shifted to the desired location. However, it is challenging to regulate an outer section when the output of the inner loop varies frequently. For attaining better dynamic qualities of the systems under control, the fuzzy cascade controller's variables are optimised. As a result, an enhanced performance has been obtained by the modified membership functions.

2.4. Grid synchronization in single phase PV system

Grid detection and synchronisation play a significant role in the control system of a single-phase grid connected PV panel, which is depicted in Figure 6. As a precautionary measure, the detecting and synchronizing technique responds to abnormal circumstances instantly when non-linear load is employed at PCC that could lead to a reduction at the point. Consequently, it is necessary to develop a rapid and accurate synchronizing approach for providing precise reference signals using potential drop within a set period. The two main categories of synchronisation techniques are PLL technique and mathematical analysis approach. The PLL approach based on adaptive filtering is the one which receives the most attention among these. Figure 7 illustrates a fundamental PLL.

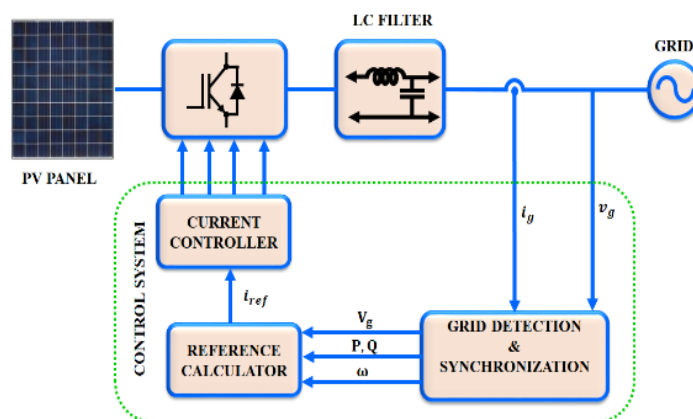


Figure 6. Control structure of 1Φ grid connected PV system

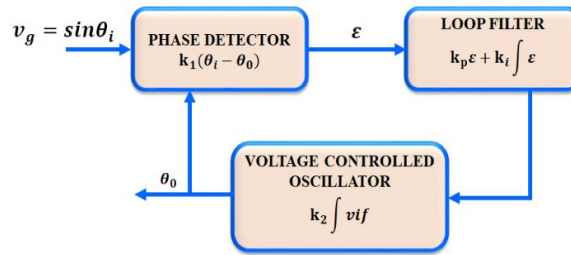


Figure 7. Basic PLL structure

PD, LP, and VCO are all components of the PLL structure. A small signal representation of 1Φ PLL becomes a second order scheme with using first order LPF, which is denoted by (15).

$$\frac{\theta_o(s)}{\theta_i(s)} = \frac{K_1 K_2 G_{lf}(s)}{s + K_1 K_2 G_{lf}(s)} = \frac{K_1 K_2 K_p s + K_1 K_2 K_i}{s^2 + K_1 K_2 K_p s + K_1 K_2 K_i} \quad (15)$$

Where, output and input phases are indicated by $\theta_o(s)$ and $\theta_i(s)$ along with gains for a voltage-controlled oscillator and phase detector are denoted by the characters K_1 and K_2 . The loop factors' transfer function is specified as (16).

$$G_{lf}(s) = K_p + K_i/s \quad (16)$$

Here, K_p, K_i symbolises loop factor's proportional and integral gains. In (12) yields the following values for damping ratio and un-damped natural frequency as.

$$\zeta = \frac{1}{2} \frac{K_p}{\sqrt{K_i}}, \omega_n = \sqrt{K_i} \quad (17)$$

The time of settling is achieved as (18) when $K_1 = K_2 = 1$.

$$t_s = \frac{4.6}{\zeta \omega_n} \quad (18)$$

Thus, another technique for phase detection which self-adjusts output utilising a feedback loop is the employment of adaptive filters.

3. RESULTS AND DISCUSSION

Grid voltage levels can vary, especially in regions with unstable or fluctuating grid conditions. The SEPIC-Luo converter efficiently handles a wide range of input voltages, allowing for grid-tied operation even in challenging grid environments. The overall proposed work is examined using MATLAB and the parameters utilized to design the proposed research are shown in Table 2.

	Parameter	Specification
Solar PV system	Series connected solar PV cells	36
	Open circuit voltage	12 V
	Short circuit current	8.33 A
	Peak Power	10 KW, 10 Panels
Integrated SEPIC-Luo	L_1, L_2	5 mH
	C_1, C_2	25 μ F
	Switching frequency	100 KHZ

In Figure 8, the temperature and irradiance waveform exhibited by PV system illustrated. It is shown that a steady temperature of 25 °C is maintained initially, and that after 0.2 s the temperature rises to 35 °C due to the intermittent nature and remains stable at that level. Corresponding to the temperature a constant of 750 solar radiation.

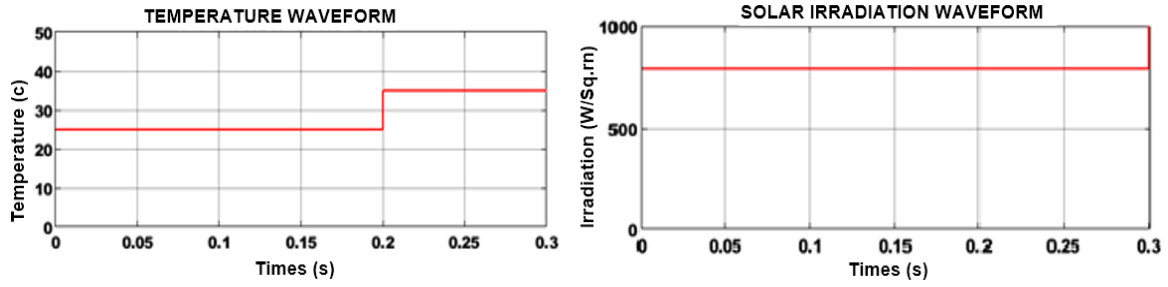


Figure 8. PV panel parameters

The waveform displayed Figure 9, demonstrates an input parameters like power, voltage, and current generated by solar PV system. The generated PV outputs are fed as input to the SEPIC-Luo converter. From figure it is observed that, with minor distortion at initial stages a constant voltage of 120 V is maintained, and after 0.2 s the voltage increases to 140 V and sustain the same throughout the system. Similarly, with rise in power a constant of 4500 W power is sustained till 0.2 s with fluctuations and after gets increased to 5900 W and continue till 0.25 s and later gets distorted. In correspondence, the converter input current rises to a peak of 20 A and retained to continue at 17 A till 0.2 s. Afterwards, current gets rises to 18 A and tends to continue till 0.25 s and later gets distorted.

The outputs of SEPIC-Luo converter in correspondence to the input parameters is shown in Figure 10. Generally, the converter boosts the voltage generated by the PV system. Here, with minor distortions at the initial stage, the output power gets increased to 4500 W at 0.2 s and gets distorted later. Similarly, the converter boosts the voltage with the assistance of cascaded fuzzy MPPT approach and a constant of 300 V is maintained throughout the system. In contrast, with peak rise in current of 18 A, a constant of 6 A is maintained with minor distortions till 0.2 s. After a constant of 7 A is sustained till 0.25 s and after gets distorted.

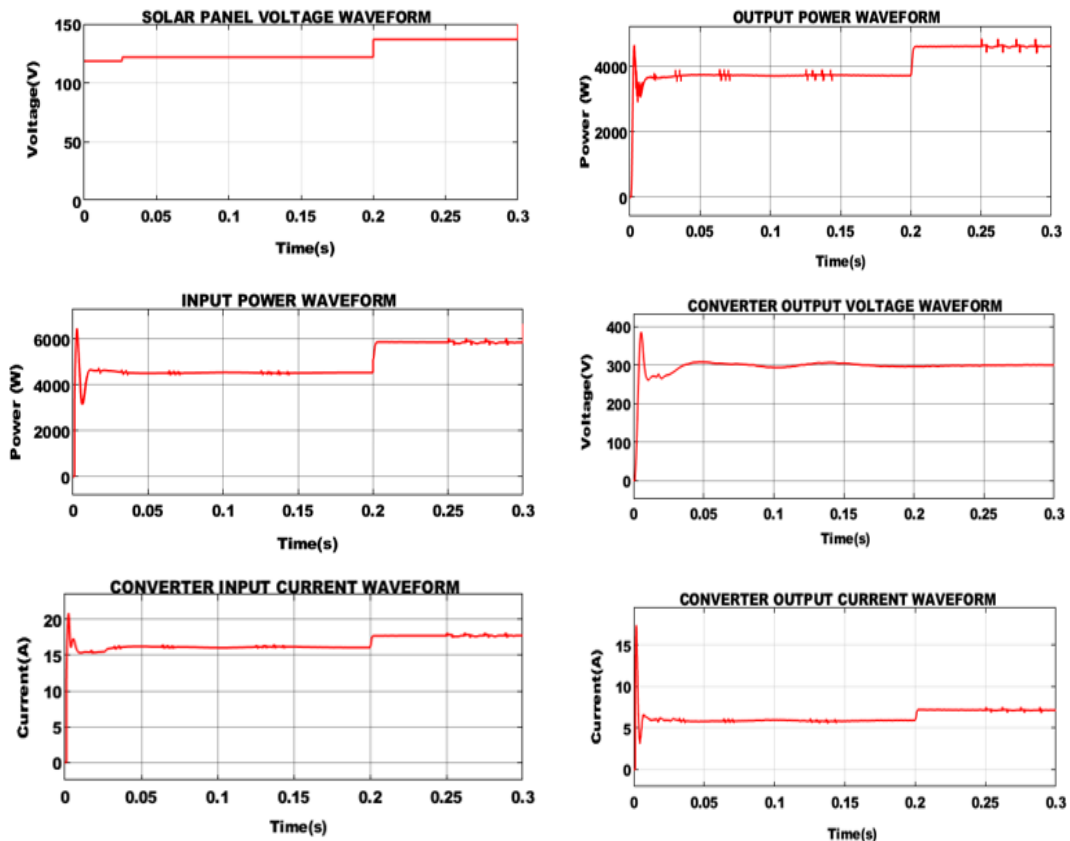


Figure 9. Input parameters of SEPIC-Luo converter

Figure 10. Converter output waveforms

Real and reactive power obtained with an assistance of PI controller is demonstrated as waveforms in Figures 11(a) and 11(b) respectively. The real power drops initially, and increases at 0.03 s and after 0.05 s a constant of 500 W reference power is obtained as shown in Figure 11(a). Subsequently, in the reactive power waveform shown in Figure 11(b), it is observed that with peak rise in power a minimized reactive power is sustained throughout the system, corresponding to real power.

Grid waveform representing voltage is shown in Figure 12(a), with a reference of 500 W. It is observed that, 230 V constant voltage is achieved in correspondence to 500 W. Similarly, grid current waveform is provided in Figure 12(b) which indicates a constant grid current of 10 A.

The grid THD of a proposed work is illustrated as bar chart in Figure 13. It is noticed that with the support of PI controller on the grid side a reduced THD of 2.91% is maintained. The efficiency and voltage gain integrated SEPIC-Luo converter in contrast to other converter approaches is illustrated in Figures 14(a) and 14(b). From Figure 14(a), it is noticed that, SEPIC-Luo converter shows improved efficiency of 96% and Figure 14(b) denotes that the converter contributes a voltage gain of 1:12 in comparison to converters like Boost, Cuk, SEPIC, and Luo converters.

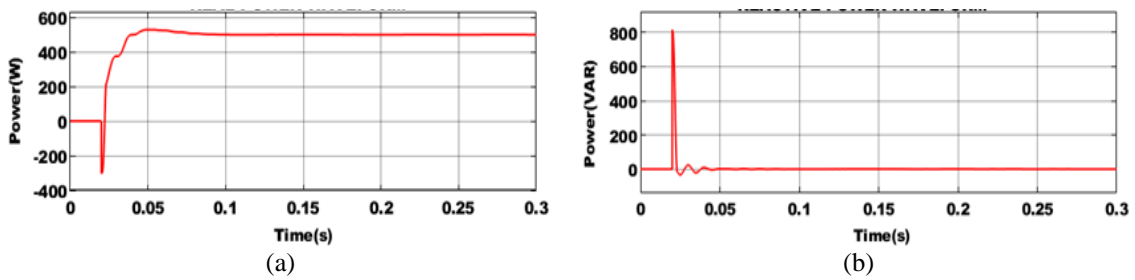


Figure 11. Waveforms for (a) real power and (b) reactive power

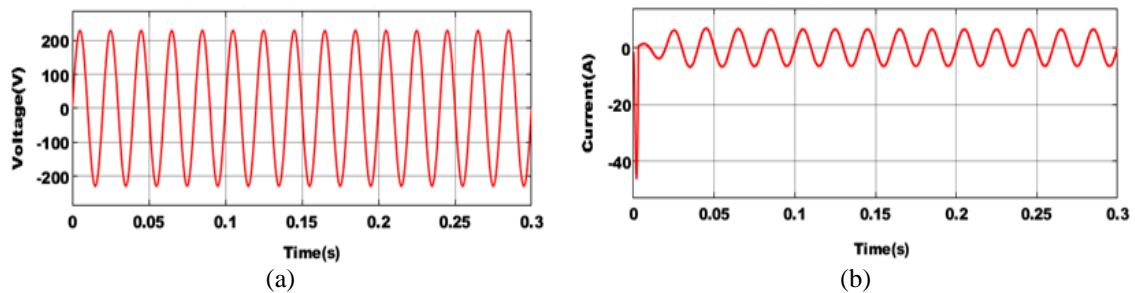


Figure 12. Grid waveforms (a) voltage and (b) current with 500 W reference

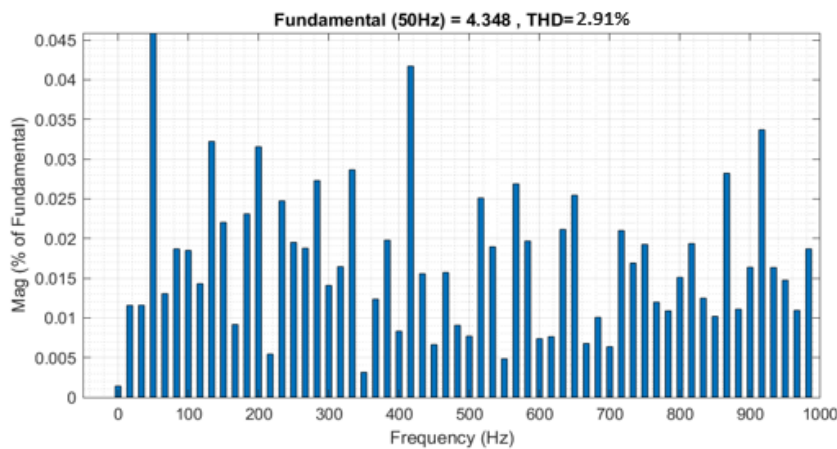


Figure 13. Grid THD waveform

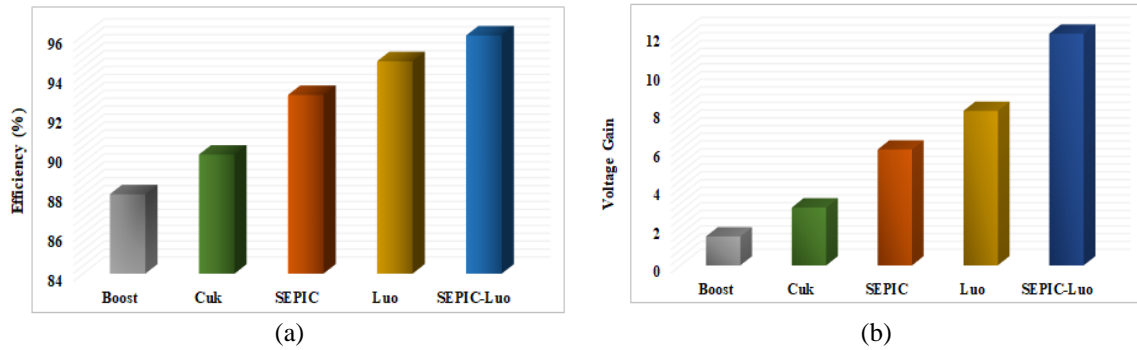


Figure 14. Comparison of (a) efficiency and (b) voltage gain

4. CONCLUSION

The ability to locate PV arrays more easily than a traditional power plant allows for the construction of solar power plants where they are essentially needed in grid system. An inefficient output voltage from PV system is sent through a SEPIC-Luo converter, which boosts the output to match the input voltage's polarity with the assistance of cascaded fuzzy MPPT controller. Better voltage gain is provided while switching losses are kept to a minimum. For analyzing the error signal and maintaining the steady state error, a closed loop PI controller is used. The outputs reveal that the proposed system contributes less distortion delivering reliable power by effective grid synchronization. Simulated outputs using MATLAB/Simulink provides voltage gain of 1:12 with improved efficiency of 96% respectively. Future work involves further enhancing the system's performance by fine-tuning control strategies, optimizing the system responds to different conditions. Additionally, integrating energy storage solutions can contribute to improved stability by mitigating fluctuations and providing backup during low sunlight periods, thereby enhancing the overall reliability of the power generation system. This comprehensive approach ensures a more robust and consistent energy output, aligning with the demands of a stable and efficient renewable energy system.




REFERENCES

- [1] Z. Shi, W. Wang, Y. Huang, P. Li, and L. Dong, "Simultaneous optimization of renewable energy and energy storage capacity with the hierarchical control," *CSEE Journal of Power and Energy Systems*, vol. 8, no. 1, pp. 95–104, 2022, doi: 10.17775/CSEEJPES.2019.01470.
- [2] N. Haegel and S. Kurtz, "Global progress toward renewable electricity: tracking the role of solar," *IEEE Journal of Photovoltaics*, vol. 11, no. 6, pp. 1335–1342, Nov. 2021, doi: 10.1109/JPHOTOV.2021.3104149.
- [3] M. S. Hossain, A. Jahid, K. Z. Islam, and M. F. Rahman, "Solar PV and biomass resources-based sustainable energy supply for off-grid cellular base stations," *IEEE Access*, vol. 8, pp. 53817–53840, 2020, doi: 10.1109/ACCESS.2020.2978121.
- [4] S. A. Nabavi, N. H. Motlagh, M. A. Zaidan, A. Aslani, and B. Zakeri, "Deep learning in energy modeling: application in smart buildings with distributed energy generation," *IEEE Access*, vol. 9, pp. 125439–125461, 2021, doi: 10.1109/ACCESS.2021.3110960.
- [5] L. Jia, J. Ma, P. Cheng, and Y. Liu, "A perspective on solar energy-powered road and rail transportation in China," *CSEE Journal of Power and Energy Systems*, vol. 6, no. 4, pp. 760–771, 2020, doi: 10.17775/CSEEJPES.2020.02040.
- [6] I. Akhtar, S. Kirmani, M. Jameel, and F. Alam, "Feasibility analysis of solar technology implementation in restructured power sector with reduced carbon footprints," *IEEE Access*, vol. 9, pp. 30306–30320, 2021, doi: 10.1109/ACCESS.2021.3059297.
- [7] I. Akhtar, S. Kirmani, and M. Jameel, "Reliability assessment of power system considering the impact of renewable energy sources integration into grid with advanced intelligent strategies," *IEEE Access*, vol. 9, pp. 32485–32497, 2021, doi: 10.1109/ACCESS.2021.3060892.
- [8] A. Moghasssemi, S. Padmanaban, V. K. Ramachandramurthy, M. Mitolo, and M. Benbouzid, "A Novel Solar Photovoltaic Fed TransZSI-DVR for power quality improvement of grid-connected PV systems," *IEEE Access*, vol. 9, pp. 7263–7279, 2021, doi: 10.1109/ACCESS.2020.3048022.
- [9] B. Chandrasekar *et al.*, "Non-isolated high-gain triple port DC–DC buck-boost converter with positive output voltage for photovoltaic applications," *IEEE Access*, vol. 8, pp. 113649–113666, 2020, doi: 10.1109/ACCESS.2020.3003192.
- [10] R. Panigrahi, S. K. Mishra, S. C. Srivastava, A. K. Srivastava, and N. N. Schulz, "Grid integration of small-scale photovoltaic systems in secondary distribution network—a review," *IEEE Transactions on Industry Applications*, vol. 56, no. 3, pp. 3178–3195, May 2020, doi: 10.1109/TIA.2020.2979789.
- [11] J. Ahmad *et al.*, "Performance analysis and hardware-in-the-loop (HIL) validation of single switch high voltage gain DC-DC converters for MPP tracking in solar PV system," *IEEE Access*, vol. 9, pp. 48811–48830, 2021, doi: 10.1109/ACCESS.2020.3034310.
- [12] A. El Aroudi, R. Haroun, M. Al-Numay, and M. Huang, "Multiple-loop control design for a single-stage PV-fed grid-tied differential boost inverter," *Applied Sciences*, vol. 10, no. 14, p. 4808, Jul. 2020, doi: 10.3390/app10144808.
- [13] I. Jagadeesh and V. Indragandhi, "Comparative study of DC-DC converters for solar PV with microgrid applications," *Energies*, vol. 15, no. 20, p. 7569, Oct. 2022, doi: 10.3390/en15207569.
- [14] H. F. Feshara, A. M. Ibrahim, N. H. El-Amary, and S. M. Sharaf, "Performance evaluation of variable structure controller based on sliding mode technique for a grid-connected solar network," *IEEE Access*, vol. 7, pp. 84349–84359, 2019, doi: 10.1109/ACCESS.2019.2924592.
- [15] B. R. Ananthapadmanabha, R. Maurya, and S. R. Arya, "Improved power quality switched inductor Cuk converter for battery charging applications," *IEEE Transactions on Power Electronics*, vol. 33, no. 11, pp. 9412–9423, Nov. 2018, doi: 10.1109/TPEL.2018.2797005.




- [16] K. Nathan, S. Ghosh, Y. Siwakoti, and T. Long, "A new DC–DC converter for photovoltaic systems: coupled-inductors combined Cuk-SEPIC converter," *IEEE Transactions on Energy Conversion*, vol. 34, no. 1, pp. 191–201, Mar. 2019, doi: 10.1109/TEC.2018.2876454.
- [17] H. Ardi and A. Ajami, "Study on a high voltage gain SEPIC-based DC–DC converter with continuous input current for sustainable energy applications," *IEEE Transactions on Power Electronics*, vol. 33, no. 12, pp. 10403–10409, Dec. 2018, doi: 10.1109/TPEL.2018.2811123.
- [18] B. Faridpak, M. Farrokhifar, M. Nasiri, A. Alahyari, and N. Sadoogi, "Developing a super-lift Luo-converter with integration of buck converters for electric vehicle applications," *CSEE Journal of Power and Energy Systems*, vol. 7, no. 4, pp. 811–820, 2020, doi: 10.17775/CSEEJPES.2020.01880.
- [19] C. Yanarates, Y. Wang, and Z. Zhou, "Unity proportional gain resonant and gain scheduled proportional (PR-P) controller-based variable perturbation size real-time adaptive perturb and observe (P&O) MPPT algorithm for PV systems," *IEEE Access*, vol. 9, pp. 138468–138482, 2021, doi: 10.1109/ACCESS.2021.3119042.
- [20] H. H. H. Mousa, A.-R. Youssef, I. Hamdan, M. Ahamed, and E. E. M. Mohamed, "Performance assessment of robust P&O algorithm using optimal hypothetical position of generator speed," *IEEE Access*, vol. 9, pp. 30469–30485, 2021, doi: 10.1109/ACCESS.2021.3059884.
- [21] A. K. Gupta *et al.*, "Effect of various incremental conductance MPPT methods on the charging of battery load feed by solar panel," *IEEE Access*, vol. 9, pp. 90977–90988, 2021, doi: 10.1109/ACCESS.2021.3091502.
- [22] M. Dehghani, M. Taghipour, G. B. Gharehpetian, and M. Abedi, "Optimized fuzzy controller for MPPT of grid-connected PV systems in rapidly changing atmospheric conditions," *Journal of Modern Power Systems and Clean Energy*, vol. 9, no. 2, pp. 376–383, 2021, doi: 10.35833/MPCE.2019.000086.
- [23] T. Wu, Y. Zheng, Q. Liu, G. Sun, X. Wang, and X. Li, "Continuous commutation failure suppression method based on self-adaptive auto-disturbance rejection proportional-integral controller for HVDC transmission system," *Journal of Modern Power Systems and Clean Energy*, vol. 8, no. 6, pp. 1178–1187, 2020, doi: 10.35833/MPCE.2019.000431.
- [24] B. Cao, L. Chang, and R. Shao, "Predictive current controller for single-phase grid-connected VSIs with compensation for time-delay effect and system uncertainty," *IEEE Journal of Emerging and Selected Topics in Power Electronics*, vol. 6, no. 4, pp. 1761–1768, Dec. 2018, doi: 10.1109/JESTPE.2018.2806895.
- [25] S.-K. Oh, W.-D. Kim, and W. Pedrycz, "Design of optimized cascade fuzzy controller based on differential evolution: simulation studies and practical insights," *Engineering Applications of Artificial Intelligence*, vol. 25, no. 3, pp. 520–532, Apr. 2012, doi: 10.1016/j.engappai.2012.01.002.

BIOGRAPHIES OF AUTHORS






D. Thivya Prasad    received his Bachelor of Engineering degree in Electronics and Instrumentation Engineering from Mookambigai College of Engineering, Pudukkottai, India; his Master of Technology degree in Power Electronics and Drives from SASTRA University, Thanjavur, India, and Pursuing Ph.D. in Annamalai University, Chidambaram, India. He is a research scholar in Department of Electrical and Electronics Engineering, Faculty of Engineering and Technology at Annamalai University, Chidambaram, Tamil Nadu, India. His current research interests include renewable energy and power electronics. He can be contacted at email: dthivyaprasad45@gmail.com.



Dr. R. Anandhakumar    received the B.E degree in Electrical and Electronics Engineering and the M.E degree in Power Systems with distinction from Annamalai University, Tamil Nadu, India in the year 2000 and 2008 respectively. He received the Ph.D. degree in Electrical Engineering from Annamalai University, Annamalai Nagar, India in the year 2011. He published 30 research articles in various referred international journals, national journals, international conferences and national conferences. He guided one PhD student and three ongoing students to his credit. His areas of research interests include power system operation and control and computational intelligence applications. He is a Fellow of Institution of Engineers (India). He is presently working as Assistant Professor in Department of Electrical and Electronics Engineering, Faculty of Engineering and Technology at Annamalai University, Chidambaram, Tamil Nadu, India. He can be contacted at email: anand_r1979@yahoo.com.



Dr. P. Balamurugan    obtained both his Bachelor's Degree in Electrical and Electronics Engineering and Master's Degree in Power Electronics and Drives from Bharathidasan University. He has completed his Ph.D. in Development of Optimal Hybrid Energy Systems for rural areas from National Institute of Technology, Calicut, Kerala. He is presently working as Professor at Mount Zion College of Engineering and Technology, Pudukkottai India. His current research interests include renewable energy and power electronics. He can be contacted at email: principal@mountzion.ac.in.